Journal of Physics: Conference Series **582** (2015) 012036 doi:10.1088/1742-6596/582/1/012036

Performance evaluation of a digital mammography unit using a contrast-detail phantom

J Elizalde-Cabrera and M-E Brandan

Instituto de Física, Universidad Nacional Autónoma de México, Ciudad Universitaria, México DF 04510, Mexico

E-mail: brandan@fisica.unam.mx

Abstract. The relation between image quality and mean glandular dose (MGD) has been studied for a Senographe 2000D mammographic unit used for research in our laboratory. The magnitudes were evaluated for a clinically relevant range of acrylic thicknesses and radiological techniques. The CDMAM phantom was used to determine the contrast-detail curve. Also, an alternative method based on the analysis of signal-to-noise (SNR) and contrast-to-noise (CNR) ratios from the CDMAM image was proposed and applied. A simple numerical model was utilized to successfully interpret the results. Optimum radiological techniques were determined using the figures-of-merit $FOM_{SNR}=SNR^2/MGD$ and $FOM_{CNR}=CNR^2/MGD$. Main results were: the evaluation of the detector response flattening process (it reduces by about one half the spatial non-homogeneities due to the X-ray field), MGD measurements (the values comply with standards), and verification of the automatic exposure control performance (it is sensitive to fluence attenuation, not to contrast). For 4-5 cm phantom thicknesses, the optimum radiological techniques were Rh/Rh 34 kV to optimize SNR, and Rh/Rh 28 kV to optimize CNR.

1. Introduction

In order to optimize the benefits of a mammographic study, mammography systems must operate under highly controlled technical conditions, providing the necessary image quality and the minimum dose consistent with the clinical goal. Figures of merit have been defined in order to quantify the ratio between benefit and risk [1-4]. For mammographic studies, the benefit is expressed by image quality parameters, while risk is associated with mean glandular dose.

In this work we have studied image quality parameters (determined using the CDMAM phantom) and mean glandular dose delivered by a flat panel digital mammography system for different polymethyl methacrylate (PMMA) thicknesses within a range of clinically relevant radiological techniques. We´ve proposed a method to quantify image parameters which extends the contrast-detail relation offered by the phantom design. The aim has been to evaluate the system performance, find the optimum operational conditions, and compare with those selected by the system. This evaluation is needed as a benchmark for the reliable use of the unit in the current laboratory research projects.

1. Materials and methods

The analyzed system was a GE Senographe 2000D, with a dual-track (Mo-Rh) anode, and Mo (0.030 mm) and Rh (0.025 mm) filters. The digital detector consists of a 19x23 cm^2 columnar CsI(Tl) scintillator coupled to an a-silicon plate, with nominal pixel size equal to 100 μm. Raw ("for processing") images were used, unless specified. Two types of phantoms were used: homogeneous PMMA plates of various thicknesses and sufficiently large to completely cover the detector, and the CDMAM (version 3.4) [6]. The CDMAM phantom, shown in Fig 1, consists of a 0.5 mm thick aluminum base (99.5% pure Al), with 410 gold disks (99.999% pure Au) having diameters between 0.06 and 2.00 mm and thicknesses between 0.03 and 2.0 μm. A 5 mm thick, 16 x 24 cm^2 PMMA plate covers the base, and the CDMAM structure is equivalent to 1.0 cm of PMMA for a standard Mo/Mo/28 kV mammography X-ray spectrum. The phantom includes same area additional PMMA plates to simulate various breast thicknesses.

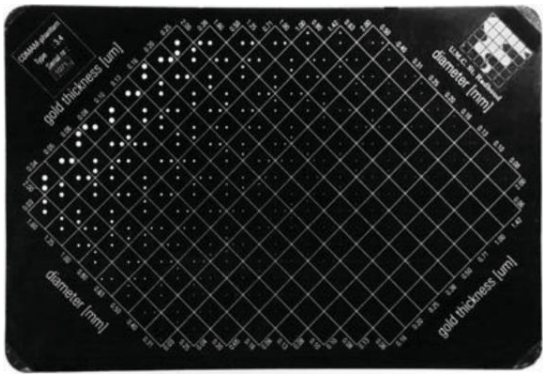

Figure 1. CDMAM phantom [5]. The 205 cells contain two gold disks each, one at the center and one placed randomly in a corner.

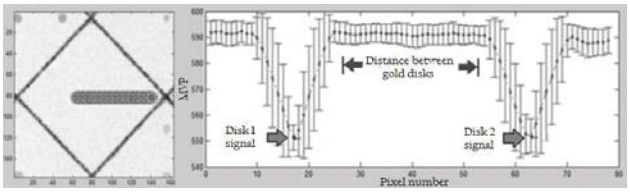

Figure 2. A typical CDMAM cell, where circular ROIs are created along the line that connects the disks. MPV and standard deviation are measured in the ROIs.

2.1 Detector response, and uniformities of the detector and X-ray field

The detector response was evaluated as the relation between mean pixel value (MPV) and X-ray tube mAs in images of a 4.5 mm thick PMMA phantom for Mo/Mo 28 kV X-rays at manually selected mAs values. MPV was obtained in squared 4 cm^2 regions-of-interest (ROIs) centered 6 cm from the torax edge of the image.The relation should be linear (squared correlation coefficient $R^2 > 0.99$).

The detector uniformity was evaluated [5], acquiring raw images of a 4.5 cm thick PMMA phantom. The MPV was measured in squared ROIs at the center and corners of the phantom image. The relative MVP deviation of any ROI from the average should be < ±15%.

The uniformity of the X-ray field was determined exposing radiochromic film (EBT3 GrafChromic) to the appropriate air-kerma to induce a response (about 0.5 Gy) under the same X-ray conditions as the previous test. The film was located 15 cm above the breast support base and normal to the beam direction. The film was digitized before and after the exposure in order to extract the net response by subtraction [7-8]. A flatbed HP Scanjet 7650 with 300 ppm resolution was used.

2.2 Measurement of image quality and mean glandular dose

CDMAM images were acquired with the phantom placed on top of 2 cm thick PMMA in order to keep a constant distance between phantom and detector. Total phantom thicknesses were 4.0, 4.5 and 5.0 cm. All anode/filter combinations, voltage between 25 and 34 kV, and three mAs values for each combination were analyzed; 8 images were acquired for each setting. Also, images for each CDMAM thickness were obtained under automatic exposure control (AEC).

The evaluation of image quality was performed in the traditional way, using the *CDMAM Analyser v1.5.3* [9] code, and a custom-made Matlab-based software. The first provided contrast-detail curves where the threshold disk thickness visible in the phantom image was evaluated for each disk diameter. The second code evaluated standard image quality parameters from the CDMAM images. These indicators were signal, noise, signal-to-noise ratio (SNR), contrast, and contrast-to-noise ratio (CNR), measured in individual phantom cells chosen by the user. The code locates the center of each disk in the cell, draws a straight line between them, and generates circular ROIs of the same diameter as the analyzed disks. Inside the ROIs, MPV and standard deviation are calculated. A MPV profile is created, as shown in Fig. 2, and the average MPV in both disks and the cell noise are obtained from the profile. From these, SNR and CNR are also calculated.

Mean glandular dose MGD was calculated for each PMMA thickness following Dance [10**,** 11],

$$MGD = K_{ES} g c s \,, \tag{1}$$

where K_{ES} is air-kerma at the phantom entrance surface, g is a factor that converts air-kerma into dose for 50% glandularity, c is a factor that corrects for differences in glandularity, and s is a factor that corrects for anode/filter combinations other than Mo/Mo. The radiological technique was the one chosen by the unit AEC.

2.3 Figures-of-merit (FOM)

Two figures-of-merit, FOM_{SNR} for SNR and FOM_{CNR} for CNR, were calculated as follows.

$$FOM_{SNR} = \frac{SNR^2}{MGD}\,,\ FOM_{CNR} = \frac{CNR^2}{MGD}\,. \tag{2}$$

In principle, these are independent of the photon fluence and depend on beam quality only.

2.4 Calculation of signal and noise

Detector signal and noise were numerically calculated following Lemacks' formalism [12] which includes knowledge of the spectrum, attenuation, detector efficiency and transformation of X-rays into light. From signal and noise, SNR and CNR were obtained. Fig 3 shows the calculation geometry.

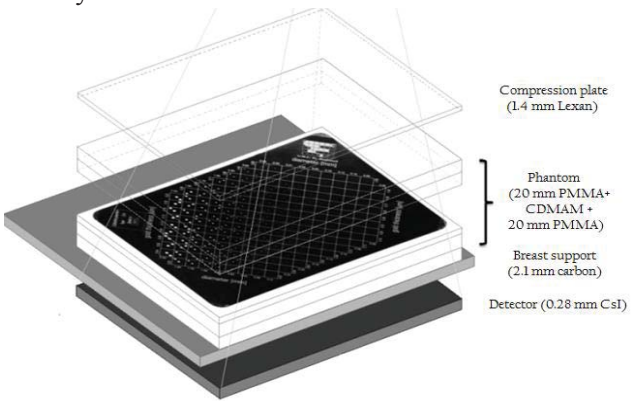

Figure 3. Geometry for numerical calculations. The focal spot is 66 cm from the detector, towards the top.

3. Results

3.1 Detector response, and uniformities of the detector and X-ray field

The detector response was lineal, R^2= 0.99991. Figure 4(A) shows the X-ray intensity distribution for Mo/Mo at 28 kV, and Fig 4 (B), the pixel value distribution for the same technique. The radiation field showed a maximum next to the thorax edge, slightly to the right, and a minimum at the superior left corner. The difference between the extreme values was ≈ 18%.The flat field pixel

image showed a maximum at the center, slightly to the left and a minimum at the top right corner. The difference between extrema was ≈ 8%. Similar X-ray and detector distributions were measured for Rh/Rh.

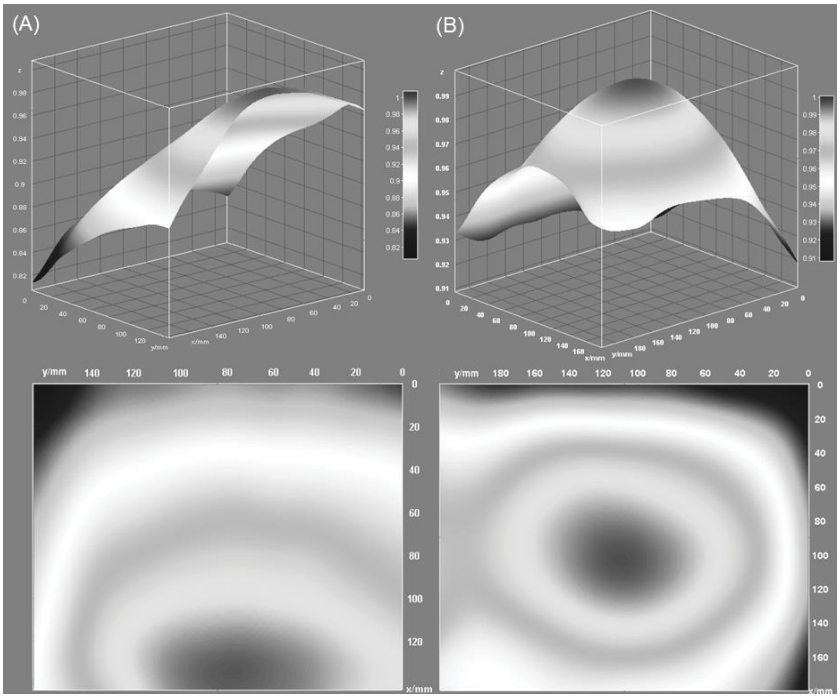

Figure 4. (A) X-ray intensity distribution measured with radiochromic film, normalized to its maximum for Mo/Mo, 28 kV. (B) Raw image pixel value normalized distributions for the same technique.

3.2 Measurement of image quality and mean glandular dose

Measured mean glandular doses were 1.2, 1.1 and 1.1 mGy for PMMA thicknesses of 4.0, 4.5 and 5.0 cm, equivalent to 4.5, 5.3 and 6.0 cm thick compressed breasts. These values comply with international recommendations [6]. The radiological techniques chosen by the AEC for 4.0, 4.5 and 5.0 cm PMMA were Mo/Mo, Mo/Rh, and Rh/Rh, all at 28 kV, respectively.

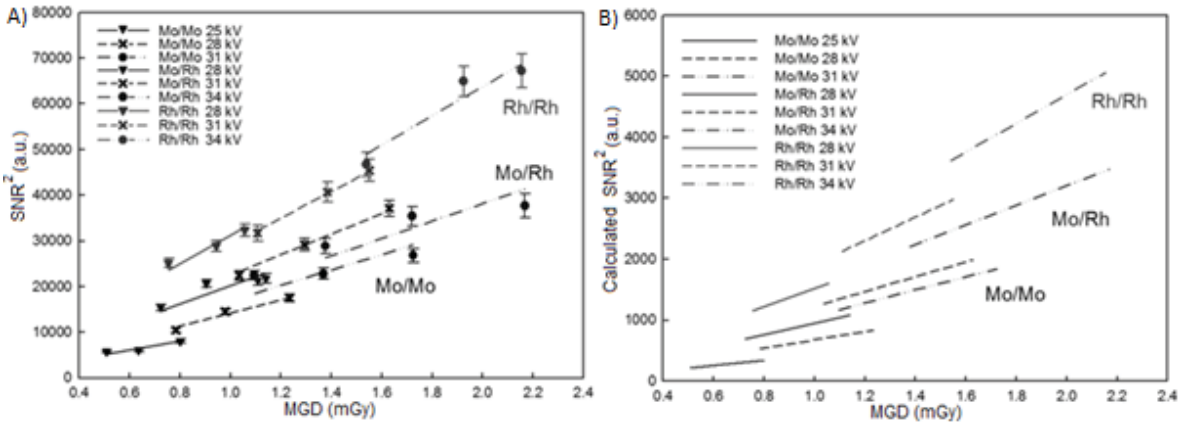

Figure 5. A) Measured SNR^2 vs MGD for a 4.5 cm thick PMMA phantom. All the analyzed anode/filter combinations and voltages are shown. B) Calculations for the same magnitudes.

Figure 5, left, shows representative values of SNR^2 and MGD measured for a 4.5 cm thick PMMA phantom. At the right, the corresponding calculations, which describe well the measurements.

3.*3 Figures-of-merit*
For 4.0 and 5.0 cm PMMA thicknesses, optimum FOM_{SNR} were obtained for the Rh/Rh beams and for 4.0 and 4.5 cm, changes in kV between 31 and 34 changed FOM_{SNR} little (only 1 to 4 %). For 5.0 cm, the optimum FOM_{SNR} was obtained at 34 kV. On the other hand, FOM_{CNR} optimization at each thickness required Rh/Rh beams at 28 kV. The unit AEC selected the optimum parameters (in terms of FOM_{CNR}) only for 5 cm PMMA.

4. Discussion and conclusions

Figures-of-merit have predicted optimum operation parameters. In general for the analyzed thicknesses, the optimum values were Rh/Rh at 34 kV for SNR and Rh/Rh at 28 kV for CNR. This result is consistent with independent conclusions such as those in [1-4]. These beams were harder (more energetic) than those automatically chosen by the unit; the AEC selected Rh/Rh only for 5 cm PMMA. The flat-fielding process preformed as a pre-process by the Senographe 2000D system reduced by about one half the non-homogeneities created by the heel effect, but the image of the homogeneous phantom still showed differences up to 6% between central and corner pixels. The MGD values for all PMMA thicknesses, which were equivalent to 4.5, 5.3 and 6.0 cm compressed breasts, respectively, were within international recommendations [5]. Analysis of both figures-of-merit indicated that the automatic control has been set to keep SNR constant, without consideration of contrast.

This overall evaluation has characterized the beam properties, delivered dose, and detector performance of this mammography unit which is currently used in research projects at our laboratory.

Acknowledgements
Authors thank C. Ruiz-Trejo and E. López-Pineda for continuous technical support during the project. We acknowledge partial financial support from DGAPA-UNAM Grant PAPIIT IN105813. JEC acknowledges a CONACyT scholarship for M.Sc.(Medical Physics) studies. We thank Miguel Rodríguez-Ponce, INCan, for facilitating the realization of this work.

References

[1] Baldelli P, Phelan N and Egan G 2008 Effect of Anode/Filter Combination on the Dose and Image Quality of a Digital Mammography System Based on an Amorphous Selenium Detector*, IWDM LNCS* **5116** 716-23
[2] Williams M B, Raghunathan P, More M J, Seibert J A, Kwan A, Lo J Y, Samei E, Ranger N T, Fajardo L L, McGruder A, McGruder S M, Maidment A D, Yaffe M J, Bloomquist A and Mawdsley G E 2008 Optimization of exposure parameters in full field digital mammography *Med. Phys.* **35** 2414-23
[3] Young K C, Cook J J H and Oduko J M 2006 Use of the European Protocol to Optimise a Digital Mammography System *IWDM LNCS* **4046** 362-9
[4] Young K C, Oduko J M, Bosmans H, Nijs K and Martinez L 2006 Optimal beam quality selection in digital mammography *The British Journal of Radiology* **79** 981-90.
[5] SEFM, SEPR and SERAM 2011 (in Spanish) Protocolo Español de Control de Calidad en Radiodiagnóstico
[6] Karssemeijer N and Thijssen M A O 1996 Determination of contrast-detail curves of mammography systems by automated image analysis *Digital Mammography* **96** 155-60
[7] Fuss M, Sturtewagen E, De Wagter C and Georg D 2007 Dosimetric characterization of GafChromic EBT film and its implication on film dosimetry quality assurance *Phys. Med. Biol.* **52** 4211-25

[8] Massillon-JL G, Chiu-Tsao S T, Domingo-Muñoz I and Chan M F 2012 Energy Dependence of the New Gafchromic EBT3 Film: Dose Response Curves for 50 KV, 6 and 15 MV X-Ray Beams *International Journal of Medical Physics, Clinical Engineering and Radiation Oncology* **1** 60-5
[9] European Reference Organisation for Quality Assured Breast Screening and Diagnostic Services, *http://www.euref.org*
[10] Dance D R 1990 Monte Carlo calculation of conversion factors for the estimation of mean glandular breast dose *Phys. Med. Biol.* **35** 1211-9
[11] Dance D R, Skinner C L, Young K C, Beckett J R and Kotre C J 2000 Additional factors for the estimation of mean glandular breast dose using UK mammography dissymmetry protocol *Phys. Med. Biol.* **45** 3225-40.
[12] Lemacks M R, Kappadath S C, Shaw C C, Liu X and Whitman G J 2002 A dual-energy subtraction technique for microcalcification imaging in digital mammography- A signal-to-noise analysis *Med. Phys.* **29** 1739-51